DOCTEUR EN SCIENCES BIOMÉDICALES ET PHARMACEUTIQUES

Biosynthèse, transport et fonction de l'hyaluronidase HYAL1 dans les macrophages et ostéoclastes murins

Puissant, Émeline

Award date:
2019

Awarding institution:
Universite de Namur

Inactivation of the hyaluronidase HYAL1 decreases bone mineral density in mice

Emeline Puissant[1], Bruno Flamion[1], Jean-Michel Vandeweerd[2], Michel Jadot[1] and Marielle Boonen[1*]

[1]URPhyM, University of Namur, Namur, Belgium

[2]URVI, University of Namur, Namur, Belgium

[*]Corresponding author

Abbreviations:

BMD: Bone Mineral Density; CTX: C-Terminal Telopeptide of type I-collagen; HA: Hyaluronic Acid; HABP: Hyaluronic Acid Binding Protein; HES: Hematoxylin Eosin Saffron; M-CSF: Macrophage Colony-Stimulating Factor; MM: Molecular Mass; PINP: Procollagen type I N-terminal propeptide; pQCT: peripheral Quantitative Computed Tomography; RANKL: Receptor Activator of Nuclear factor Kappa-B Ligand; SEM: Standard Error of the Mean; TRAP: Tartrate-Resistant Acid Phosphatase

Keywords:

HYAL1, osteoclasts, hyaluronic acid, bone remodeling, osteopenia, lysosomes

Abstract

Hyaluronic Acid (HA) is an extracellular matrix glycosaminoglycan involved in tissue hydration and joint lubrication. Depending on its molecular mass, HA also affects the proliferation, differentiation, and activity of numerous cell types. Intriguingly, our past researches highlighted that the hyaluronidase HYAL1 is strikingly upregulated (~25x) upon differentiation of bone marrow monocytes into osteoclasts. To investigate whether HYAL1 is involved in the differentiation and resorption activity of osteoclasts, and in bone remodeling in general, we analyzed several bone parameters in *Hyal1* -/- mice and studied the differentiation of bone marrow monocytes isolated from these mice into osteoclasts. These experiments revealed that 1-year-old HYAL1 deficient mice exhibit a significant decrease of bone mineral density, which is accounted for, at least partly, by elevated osteoclast numbers and by an increase of their bone resorbing activity. We also detected an accumulation of HA in *Hyal1* -/- bones and a progressive decrease of collagen synthesis by osteoblasts upon aging of the mice. We conclude that the HYAL1-mediated catabolism of HA by osteoclasts is a key process in bone remodeling, affecting both osteoclast and osteoblast function when deficient.

1. Introduction

Hyaluronic acid (HA), aka hyaluronan, is a glycosaminoglycan composed of [D-glucuronic acid β1→3 *N*-acetyl-D-glucosamine] repeats and particularly abundant in extracellular matrices. Depending on its molecular mass, HA participates in matrix viscoelasticity, cell migration, adhesion, differentiation, as well as inflammation and angiogenesis [1]. Catabolic enzymes responsible for the changes in size of HA are therefore involved in many cellular processes. The most accepted model for HA catabolism in somatic cells proposes that the glycosylphosphatidylinositol-anchored cell surface hyaluronidase HYAL2 initiates the degradation of high MM HA into smaller fragments of approximately 20 kDa, which are then endocytosed [2]. This process likely requires the anchorage of extracellular HA on the plasma membrane by HA-binding receptors such as CD44. The intracellular enzyme HYAL1 and two exoglycosidases, β-glucuronidase and β-hexosaminidase, then pursue the degradation of HA fragments in the endosomal and lysosomal system [2-6]. More recently, two additional hyaluronidases, KIAA1199 and TMEM2, have been identified although their exact role in the model of HA catabolism is not yet established [7-8].

A question that remains open is if and how hyaluronidases intervene in bone remodeling. Several experimental studies suggest that HA and HA fragments could modulate bone turnover in a size-dependent manner [9-15]. For instance, it has been shown that osteoclasts incubated *in vitro* with soluble high MM HA exhibit a decreased bone resorbing activity [10-12]. Low MM HA fragments added exogenously also affect the behavior of osteoclasts *in vitro*, but their effect is subject to controversy. Two studies point out that they promote osteoclast differentiation and resorption activity [10, 13], whereas another group found an inhibitory effect of low MM HA on these processes [14]. It is also worth noting that a broad range of HA MM can increase the proliferation, differentiation, and activity of other cell types involved in bone remodeling, including osteoblasts [15]. Hence, it is quite difficult to predict whether bone remodeling in general is influenced by the activity of hyaluronidases, and whether changes of hyaluronidase expression and/or activity level could contribute to the physiopathology of some bone defects. While it has been found that bone HA levels are altered in several pathological conditions (e.g. increased in osteogenesis imperfecta or deficiency in vitamin D, calcium or phosphate) [16, 17], the involvement of hyaluronidases in these pathologies remains unclear.

Intriguingly, we have recently found that HYAL1 is highly overexpressed upon differentiation of macrophages into osteoclasts, and that these cells secrete HYAL1 by constitutive secretion as well as by exocytosis of lysosomes [18]. These data suggest that HYAL1 could accumulate in the resorption lacuna of osteoclasts and possibly degrade HA embedded in the bone matrix. Of note, only two other lysosomal enzymes are highly upregulated upon osteoclastogenesis, i.e. cathepsin K and TRAP (Tartrate-Resistant Acid Phosphatase), which are both central actors of bone remodeling [19]. Based on this observation, we postulated that HYAL1 could be involved in this process as well. To test this

hypothesis, we investigated several bone parameters in HYAL1 deficient knockout (KO) mice and analyzed the behavior of osteoclasts differentiated *in vitro* from *Hyal1* -/- bone marrow monocytes.

2. Results

2.1. *Hyal1* -/- mice exhibit decreased bone mineral density

In humans, a deficiency in HYAL1 causes mucopolysaccharidosis IX (MPS IX), a disease identified in 4 patients to date, and characterized by the development of juvenile idiopathic arthritis (with articular pain and effusion), proliferative synovitis, and infiltration of the synovial membrane with macrophages filled with vacuoles that accumulate glycosaminoglycans [20-22]. *Hyal1* -/- mice have a normal life-span and show no gross abnormality in the main organs. So far, their joints are the only structures in which pathological alterations have been reported. Osteoarthritis is evidenced by a loss of proteoglycans in the articular cartilage of the knee and the development of osteophytes [23].

To investigate whether HYAL1 is required for proper bone remodeling, we compared the bone mineral density (BMD) of femurs in wild-type (WT) and HYAL1 deficient (*Hyal1* -/-) mice. RT-qPCR, western blotting, and HA-degradation assays have validated that HYAL1 is no longer expressed in these *Hyal1* -/- mice [18, 23]. Using peripheral Quantitative Computed Tomography (pQCT), we measured the BMD of right femurs isolated from 1-year-old male mice of both genotypes (Table 1, $n \geq 6$ per group). Three different areas of the bones were scanned. These are located at a 17.5 % and 22 % distance (metaphysis), and at a 50 % distance (diaphysis), from the knee joint space (distal end). Two-tailed Mann-Whitney U statistical tests revealed a significant decrease of the trabecular BMD in the metaphysis of *Hyal1* -/- femurs ($p < 0.01$ at 17.5 and 22 %). A significant decrease of the cortical BMD was also measured in their diaphysis ($p = 0.01$) but not in the metaphysis.

We also detected a significant decrease of the length of both right and left femurs in *Hyal1* -/- vs WT mice (with p values < 0.05 and < 0.01, respectively; Figure 1A) suggesting that the loss of HYAL1 affects the endochondral ossification. Furthermore, histological analyses revealed a significantly decreased epiphyseal plate thickness (Figure 1B), as well as a decrease of the bone area ratio relative to the total tissue area in *Hyal1* -/- femurs (Figure 1C).

Mean (mg/cm^3) ± SEM	**WT** (n = 7)	***Hyal1* -/-** (n = 6)	p value
Metaphysis (17.5 %)			
Total BMD	357.2 ± 9.2	305.7 ± 7	0.0046 **
Trabecular BMD	250.2 ± 7.7	182.7 ± 14	0.0024 **
Cortical BMD	501.0 ± 11.5	478.0 ± 7.8	0.107
Metaphysis (22 %)			
Total BMD	400.4 ± 8.7	351.7 ± 7	0.0047 **
Trabecular BMD	283.0 ± 7.8	215.1 ± 6.7	0.0012 **
Cortical BMD	545.1 ± 10.2	510.8 ± 6.3	0.051
Diaphysis (50 %)			
Cortical BMD	674.3 ± 10.4	626.8 ± 8	0.01 *

Table 1: Bone mineral density (mg/cm^3) of right femurs isolated from 1-year-old WT or *Hyal1* -/- male mice. The BMD was measured at a 17.5, 22 or 50 % distance from the distal extremity of the femurs. Two-tailed Mann-Whitney U tests were applied to the results. *: $p < 0.05$, **: $p < 0.01$

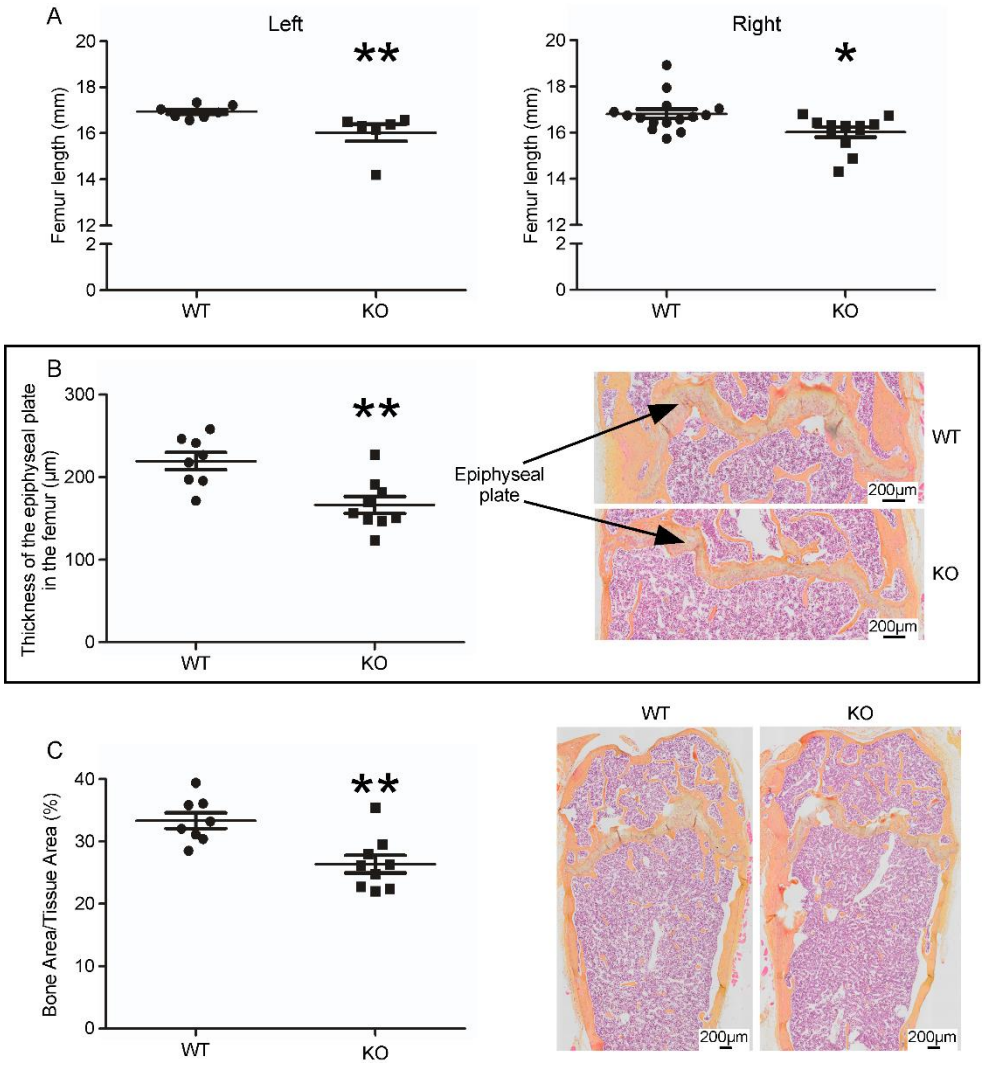

Figure 1: Femur length, thickness of the epiphyseal plate, and percentage of bone matrix in *Hyal1* -/- (KO) mice are decreased compared to WT mice. (A) Left (n ≥ 6) and right femurs (n ≥ 12) were isolated from 1-year-old mice. Their length (in mm) was measured with a digital caliper. (B) The thickness of the epiphyseal plate at the distal extremity of femurs from 18-month-old mice was quantified on 7 histological sections from each mouse. Eight measures were taken across the epiphyseal plate and averaged for each section (n ≥ 8 mice per group). (C) From the same histological slices, we calculated the percentage of bone area (light orange after hematoxylin eosin saffron coloration) compared to the total tissue area (n ≥ 8 mice in each group, 7 sections for each mouse). The graphs represent the means ± SEM. *: $p < 0.05$, **: $p < 0.01$ (two-tailed Mann-Whitney U tests).

2.2. HYAL1 deficiency causes HA accumulation in bones

We previously showed that, similarly to TRAP, WT osteoclasts cultured *in vitro* secrete large amounts of HYAL1, possibly to promote the degradation of HA in the bone matrix. To investigate whether the inactivation of *Hyal1* affects the level of HA in bone, we stained HA using HABP (HA-binding protein) on femur sections. This analysis showed a significant increase of the percentage of stained tissue in the *Hyal1* -/- mice (Figure 2A-B).

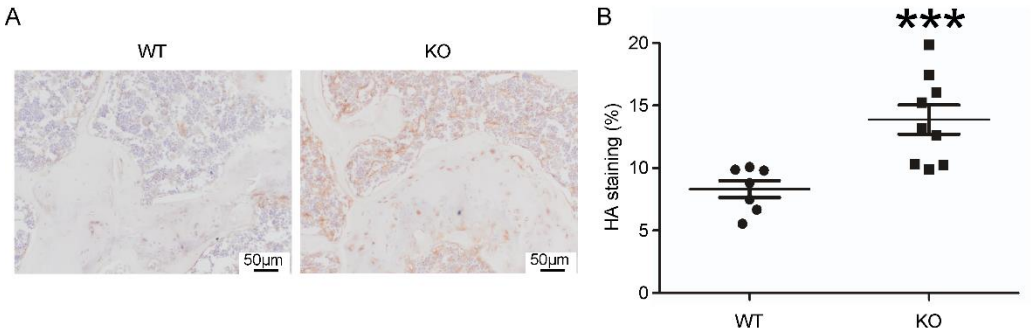

Figure 2: HA accumulates in the femurs of *Hyal1* -/- mice. (A) Histological sections of WT and *Hyal1* -/-femurs were stained for HA using HABP and counterstained with hemalun. (B) The extent of the HA staining was quantified and expressed as a percentage of the total area (in n ≥ 7 mice for each group). The graphs show the means ± SEM. ***: p< 0.001 (two-tailed Mann-Whitney U test).

Next, we assessed the mRNA level of several known actors of the metabolism of HA in WT and HYAL1 deficient osteoclasts as well as in their precursor cells. We isolated bone marrow monocytes from control and *Hyal1* -/- mice and differentiated them into osteoclasts *in vitro* in the presence of Macrophage Colony-Stimulating Factor (M-CSF) and Receptor Activator of Nuclear factor Kappa-B Ligand (RANKL). The monocytes were cultured for 5 days with M-CSF to stimulate their proliferation, survival and differentiation into macrophages [24]. Then, RANKL was added to the culture medium to induce osteoclastogenesis [25]. The mRNA expression of HYAL2, the other main hyaluronidase of somatic tissues, was decreased in *Hyal1* -/- cells, by 1.8-fold and 3.6-fold compared to the mRNA levels measured in WT macrophages and osteoclasts, respectively (Table 2). Consistent with our previous findings [18], we detected a significant increase (~ 1.9-fold) of HYAL2 mRNA level upon differentiation of WT macrophages into WT osteoclasts. This increase upon osteoclastogenesis was not detected in the *Hyal1* -/- condition.

Fold increase	*Hyal1* -/- macrophages vs WT macrophages	*Hyal1* -/- osteoclasts vs WT osteoclasts	WT osteoclasts vs WT macrophages	*Hyal1* -/- osteoclasts vs *Hyal1* -/- macrophages
HYAL2	0.55	0.27	1.87	0.63
HYAL3	3.59	3.74	2.87	2.99
CD44	1.89	1.63	0.88	1.03

Table 2: Relative mRNA expression level of HA metabolism actors in osteoclasts and bone marrow monocytes isolated from WT or HYAL1 deficient mice (n = 5).

Then, we investigated the mRNA expression of HYAL3, a protein that does not have HA-degradation activity in somatic cells but may collaborate to the activity of HYAL1 [26, 27] (Table 2). We detected a 3-fold significant increase in the mRNA level of HYAL3 in both macrophages and osteoclasts deficient for HYAL1 compared to their WT counterparts. The upregulation of HYAL3 mRNA expression detected upon osteoclastogenesis was similar for both genotypes.

Lastly, we examined the mRNA expression level of the HA receptor CD44. No significant change was seen between WT and *Hyal1* -/- cells.

Taken together, these data suggest that a deficiency of HYAL1 impairs the catabolism of HA in mouse bones, as it does in other tissues [28], without any compensatory upregulation of HYAL2. Although HYAL3 is upregulated at the mRNA level, the absence of reported activity for this hyaluronidase, and the accumulation of HA that is detected in the KO bones suggest that HYAL3 does not compensate either for the loss of HYAL1. Based on these findings, and on the observation that the HA molecules that accumulate in the serum, liver, skin, muscle, and lymph nodes of *Hyal1* -/- mice exhibit a similar MM pattern compared to HA molecules extracted from WT samples [28], we can surmise that the inactivation of HYAL1 results in an elevated concentration of total bone HA, rather than a change of its MM.

2.3. Osteoclast numbers are increased in femurs of 18-month-old *Hyal1* -/- mice, while osteoblast numbers are unchanged

To collect additional data on the bone alterations observed in *Hyal1* -/- mice, we first measured the serum levels of the osteoclast marker TRAP and of a marker of osteoclast activity, i. e. the level of C-terminal Telopeptide of type I-collagen degradation products (CTX). Neither showed any change in 7 and 18-month-old mice (Figure 3A-B).

Next, osteoclasts were identified and counted in femur sections of 18-month-old WT and KO mice through the histochemical detection of TRAP (Figure 3C). This analysis revealed that the number of osteoclasts, relative to bone perimeter, is significantly increased in *Hyal1* -/- vs WT mice both at the epiphysis and in the epiphyseal plate. We also analyzed the diaphysis, but found no difference of osteoclast numbers at this site (Figure 3D).

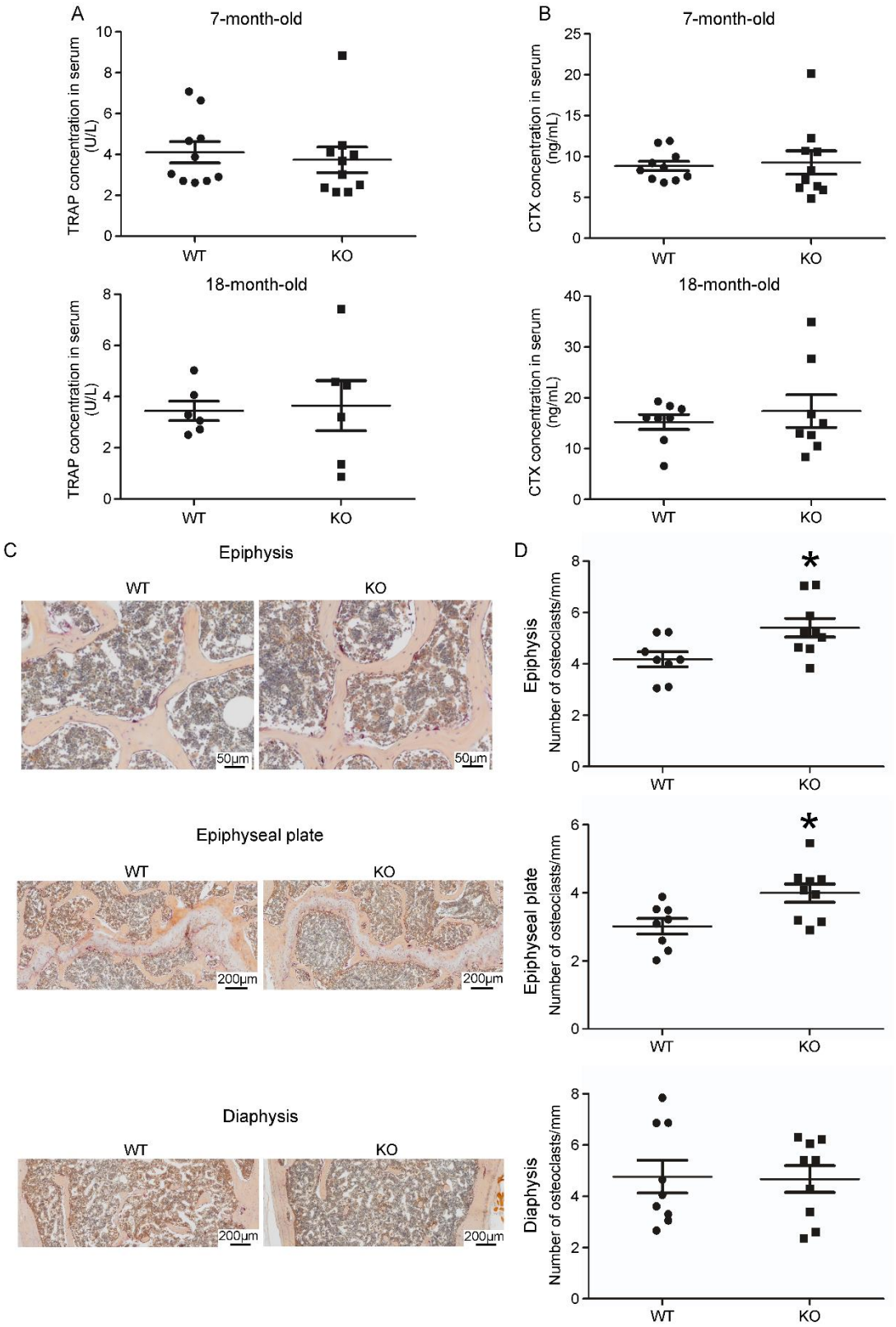

Figure 3: The number of osteoclasts is increased in *Hyal1* -/- mice compared to WT mice, even though serum levels of osteoclast markers are similar to WT levels. (A-B) TRAP (A) and CTX (B) levels were quantified using ELISA assays in the serum of 7-month (upper panel) and 18-month-old (lower panel) mice from both genotypes (n ≥ 6). (C) Representative histological sections of distal femurs from 18-month-old male *Hyal1* -/- or WT mice stained for TRAP and counterstained with hemalun. (D) The number of osteoclasts per mm of bone perimeter was counted on 2 slices for each mouse (with n ≥ 8 for each group). The quantifications were conducted at 3

different positions in the femur: the epiphysis, the epiphyseal plate, and in the diaphysis (approximately at a 25-30 % distance from the distal end). The graphs represent the means ± SEM. *: $p < 0.05$ (two-tailed Mann-Whitney U tests).

Lastly, we counted the number of osteoblasts normalized to bone perimeter on hematoxylin eosin saffron (HES) stained sections (Figure 4A). No difference was detected. In addition, we measured the plasma level of Procollagen type I N-terminal Propeptide (PINP), a marker of bone formation. While no difference was detected in 7-month-old mice, we observed a significant decrease of PINP in the plasma of 18-month-old HYAL1 deficient mice compared to control mice ($p < 0.05$, Figure 4B). Of note, a study published in 2006 did not detect any expression of HYAL1 in osteoblasts, suggesting the existence of an indirect effect of the decreased degradation of HA by osteoclasts, in which the enzyme is strongly expressed [29].

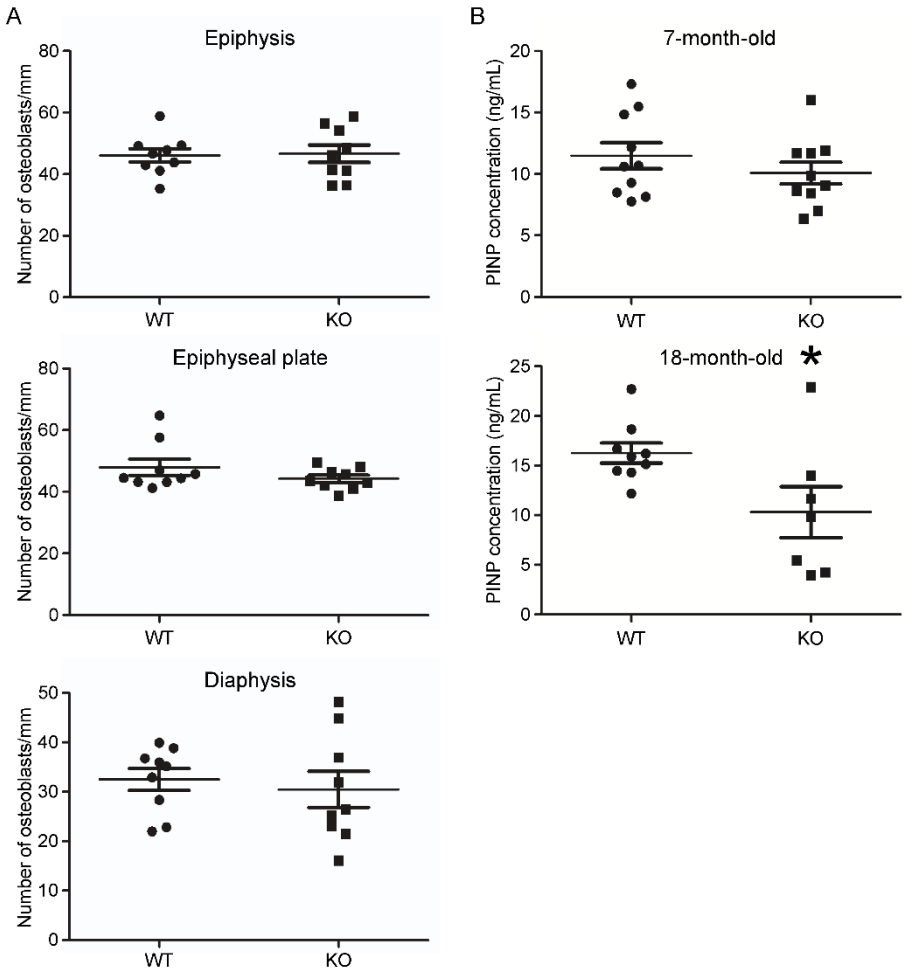

Figure 4: PINP (Procollagen type I N-terminal Propeptide) concentration is decreased in the plasma of 18-month-old *Hyal1* -/- mice compared to WT mice, with no change of osteoblast numbers in their bones. (A) The number of osteoblasts per mm of bone perimeter was quantified on HES stained slices at the epiphysis, the epiphyseal plate, and in the diaphysis (approximately at a 25-30 % distance from the distal end) (n ≥ 8 mice per group). (B) Using an ELISA assay, the concentration of PINP was measured in the plasma of 7-month (upper panel) and 18-month-old (lower panel) mice from both genotypes (n ≥ 7). The graphs show the means ± SEM. *: $p < 0.05$ (two-tailed Mann-Whitney U tests).

2.4. Inactivation of *Hyal1* does not impair the differentiation of macrophages into osteoclasts *in vitro* but potentiates osteoclast resorption activity

We pursued our investigations with an analysis of the osteoclast differentiation process and resorption activity using a combination of *in vitro* assays. In a first set of measurements, the cells were cultured on glass coverslips for 7 days in the presence of RANKL. Then, the number and size of TRAP-positive multinucleated cells (with 3 or more nuclei) were assessed. No difference was found between control and *Hyal1* -/- conditions (Figure 5A-C).

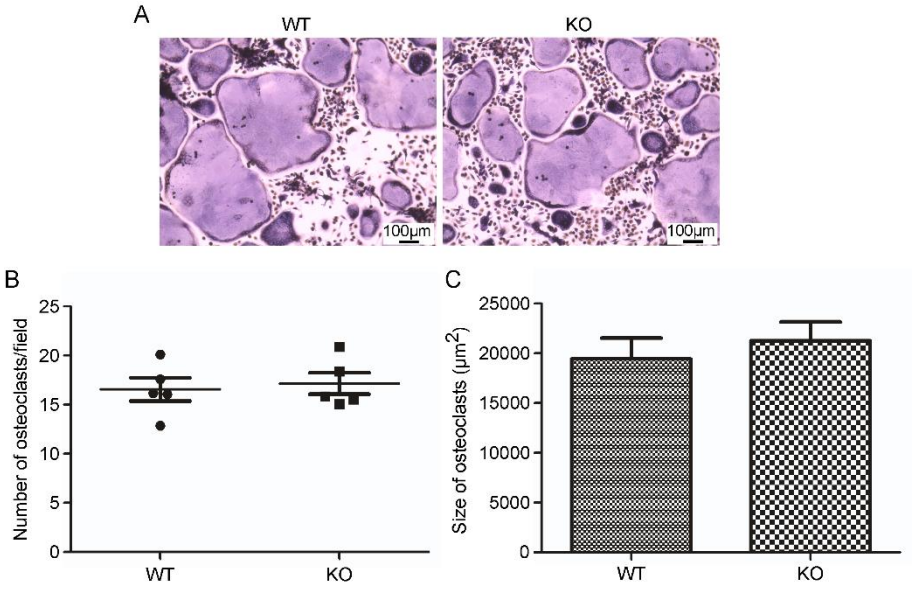

Figure 5: The loss of HYAL1 does not affect the differentiation of osteoclasts. (A) WT and HYAL1 deficient osteoclasts were differentiated for 7 days on glass coverslips before staining of the osteoclast marker TRAP. (B) The osteoclasts were counted as the number of TRAP-positive cells containing 3 or more nuclei. The quantifications were made on 25 images collected from 2 technical replicates for each mouse (n = 5 mice in each group). (C) The size of control and knockout osteoclasts differentiated on glass coverslip was measured from the average of 60 cells for each mouse (n = 5). The graphs show the means ± SEM. Two-tailed Mann-Whitney U tests indicate that there is no difference between the groups for these measurements.

In a second set of measurements, osteoclasts were differentiated on thin bone slices obtained from bovine nasal bone to assess their polarization and bone matrix resorption activity (Figure 6A) [30]. Staining of the nuclei with Hoechst 33258 and incubation with Alexa 488-phalloidin (to label the actin rings that delimit resorption lacunae) pointed out that the number of differentiated and polarized osteoclasts is similar in WT and *Hyal1* -/- conditions (Figure 6A-B). However, we detected a significant increase in the number of actin rings per field, suggesting that *Hyal1* -/- osteoclasts form more resorption lacunae than WT osteoclasts (Figure 6C). Moreover, an analysis of the bone slices by scanning electron microscopy, after removal of the cells, revealed a significant increase of the total area resorbed by *Hyal1* -/- osteoclasts compared to the area resorbed by WT osteoclasts (Figure 6D-E). Lastly, we detected a significant increase of the number of pits and of their average size in the *Hyal1* -/- condition (Figure 6F-G). Consistent with these findings, a higher amount of bone collagen degradation products (CTX) was also measured in the culture medium of *Hyal1* -/- osteoclasts differentiated on bone slices (Figure 6H). All these data point out that inactivation of HYAL1 does not affect the differentiation rate of osteoclasts but that it significantly increases their resorption activity.

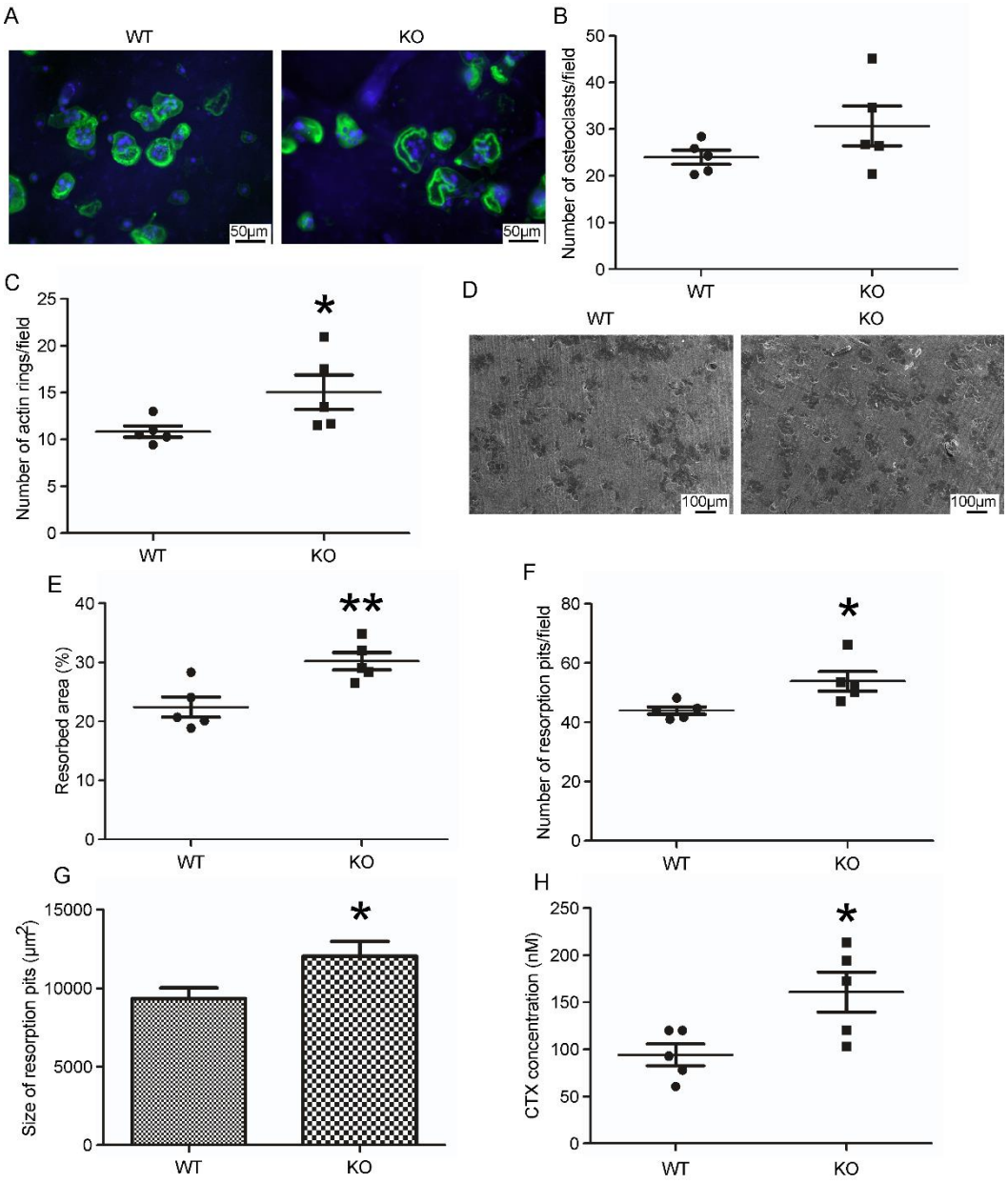

Figure 6: Inactivation of HYAL1 increases the resorption activity of osteoclasts. (A) After 10 days of differentiation on bovine bone slices, control or *Hyal1* -/- osteoclasts were fixed with paraformaldehyde. Actin rings and nuclei were then stained with Alexa 488-phalloidin and Hoechst 33258, respectively. (B) The number of polarized osteoclasts was quantified on 2 bone slices for each mouse (with n = 5 mice, and 6 images per bone slices). (C) The same images were used to count the number of actin rings per field (n = 5 mice per group). (D) After removal of the osteoclasts, the resorption pits were observed by scanning electron microscopy. (E-F) Quantifications of the percentage of the resorbed area (E) and of the number of resorption pits per field (F) were conducted based on 10 images per bone slice (with 2 bone slices for each mouse and n = 5 mice per genotype). (G) The average size of resorption pits was assessed from the measurement of at least 60 pits for each mouse (n = 5 mice per group). (H) Collagen degradation products (CTX) released from the bovine bone slices upon resorption by osteoclasts were measured in the culture supernatants using an ELISA assay. To do so, conditioned media were collected between day 8 and day 10 after plating and differentiation of the macrophages on bone slices (n = 5 mice per group, and technical replicates were quantified for all mice). The graphs show the means ± SEM. *: $p < 0.05$, **: $p < 0.01$ (two-tailed Mann-Whitney U tests).

2.5. The intracellular levels of cathepsin K and TRAP are decreased in *Hyal1 -/-* osteoclasts

To test whether the increased resorption activity of *Hyal1* -/- osteoclasts could be accounted for by an alteration of the expression of characterized actors of bone resorption, we first investigated the transcriptional expression of cathepsin K and TRAP. It is well known that the genes coding for these hydrolases are highly upregulated upon osteoclastogenesis [19]. We compared cathepsin K and TRAP mRNA levels in control and *Hyal1* -/- precursor macrophages, then in control and *Hyal1* -/- osteoclasts differentiated *in vitro* from these macrophages (for 7 days in plastic wells). No statistically significant difference was detected (supplementary table 1).

Next, we analyzed the protein expression levels of cathepsin K and TRAP by western blotting (Figure 7). These analyses revealed that the levels of mature/active forms of cathepsin K and TRAP are reduced by 30 % and 55 %, respectively, in *Hyal1* -/- vs control osteoclasts (Figure 7A-B, $p \leq 0.05$ and $p \leq 0.001$, respectively). To investigate whether these decreases correlate with the hypersecretion of cathepsin K and TRAP by *Hyal1* -/- osteoclasts, we analyzed the presence of these proteins in culture media. First, the presence of TRAP activity was measured in osteoclast lysates and in media collected after a 24 h culture period (day 6 to day 7 of differentiation process) using a colorimetric assay [31]. In accordance with the western blotting results, the intracellular activity level of TRAP was found decreased in *Hyal1* -/- cells. However, the relative amount of active TRAP secreted into the medium by WT and *Hyal1* -/- osteoclasts was found similar at steady state (Figure 7C), indicating that this enzyme is not hypersecreted by HYAL1 deficient cells.

Then, the secretion of cathepsin K was measured by western blotting only as the enzymatic assay was not sufficiently sensitive. Only a very low level of secretion, around 2 %, was found in both control and *Hyal1* -/- osteoclasts after a 4 h culture period in absence of serum, demonstrating that, as observed for TRAP, this enzyme is not hypersecreted by *Hyal1* -/- osteoclasts in this assay.

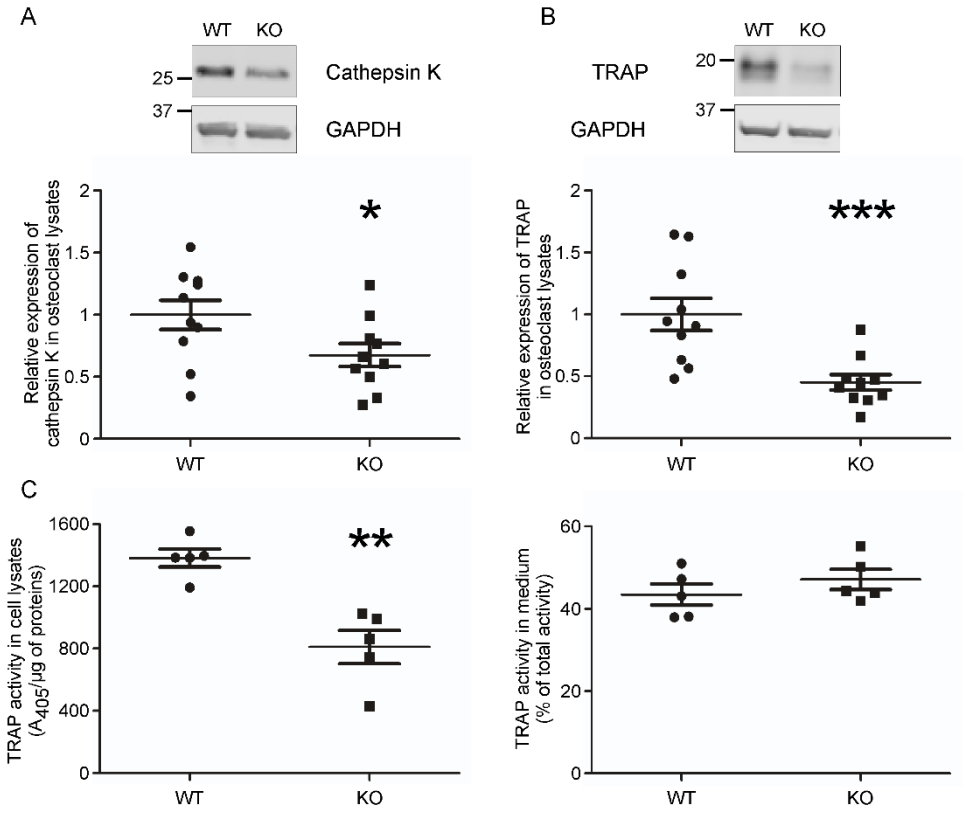

Figure 7: Protein levels of *c*athepsin K and TRAP are decreased in *Hyal1* -/- osteoclasts. Cathepsin K (A) and TRAP (B) were detected in isolated WT and HYAL1 deficient osteoclasts by western blotting after 7 days of differentiation on plastic. The signals were quantified and normalized with the housekeeping gene GAPDH. The graphs below the blots show the marker levels in *Hyal1* -/- cells relative to WT (n = 10). (C) The activity of TRAP was measured in osteoclast lysates (left panel) and in conditioned media (right panel) collected after a 24 h culture period (day 6 to day 7 of the differentiation process). The intracellular activities were normalized to the total amount of proteins in the cells. The secretion level is expressed as a percentage of total activity (activity measured in cell extracts + activity measured in the 24 h conditioned media) (n = 5). The graphs show the means ± SEM. *: $p < 0.05$, **: $p < 0.01$, ***: $p < 0.001$ (two-tailed Mann-Whitney U tests).

3. Discussion

The data presented here demonstrate that inactivation of the hyaluronidase HYAL1 in mice causes a general loss of BMD (both in cortical and trabecular bone) and impairs the longitudinal growth of bones. These findings provide the first direct evidence that this enzyme, which is strongly expressed by osteoclasts [18], plays an active role in bone physiology. There is every reason to believe that the role of HYAL1 in bone homeostasis is to degrade HA, possibly at the level of the resorption lacuna, because HYAL1 has no other known function apart from HA catabolism. Moreover, a similar decrease of long bone length is also detected in mice deficient for the hyaluronidase HYAL2 or another protein involved in HA depolymerization, KIAA1199 [32, 33].

The decrease of BMD in response to the loss of HYAL1 might seem surprising at first, considering that HYAL1 is an enzyme that degrades a bone matrix component, and that inactivation of cathepsin K or TRAP, i.e. other lysosomal enzymes involved in bone matrix degradation, results in osteopetrosis [34, 35]. However, it should be noted that the sheer amount of HA in bones is not very high as it represents at most 7 % of all glycosaminoglycans in normal bone matrix [16]. Moreover, it is well known that HA and its fragments are not simply scaffolding molecules in extracellular matrices, they affect many cellular processes. In bones more specifically, our data indicate that a HYAL1 deficiency does not modify osteoblast numbers but that it significantly hampers their ability to synthesize type I-collagen (as indicated by the lower levels of PINP in the plasma of old KO mice), consistent with the osteopenia phenotype of the *Hyal1* -/- mice. This phenotype is also accounted for by a dysregulation of osteoclasts. We detected an increase of their numbers in *Hyal1* -/- bones, as well as an increase of the bone resorption activity of *Hyal1* -/- osteoclasts differentiated *in vitro* from bone marrow monocytes and cultured on bone slices. This form of osteoclast upregulation may be due to the accumulation of non-degraded HA molecules around *Hyal1* -/- osteoclasts. Indeed, it has been demonstrated that addition of HA of different MM into the culture medium of differentiating osteoclasts can affect their differentiation rate, adhesion to the bone matrix, and resorption activity level [10-14, 36]. Albeit there are some discrepancies in these studies, low MM HA molecules (1.6 kDa up to 230 kDa) appear to have the strongest promoter effect on osteoclast differentiation and on osteoclast-mediated bone resorption [10, 13]. Whether these species accumulate in response to the HYAL1 deficiency remains to be determined.

It is worth noting that an increase of the amount of HA in the extracellular bone matrix of *Hyal1* -/- femurs could also promote bone resorption indirectly. It has been shown that HA binds to stromal cells and modulates their expression of RANKL, which controls osteoclastogenesis [37, 38]. This level of regulation by HA would not take place in the *in vitro* assay that we used to differentiate osteoclasts on bovine bone slices, which was conducted in the absence of other cell types. This could explain why *Hyal1* -/- osteoclasts numbers were found normal when the cells were differentiated *in vitro*, while increased when counted on *Hyal1* -/- bone sections.

In addition to providing much needed information regarding the relevance of the expression of hyaluronidases in bones, our findings open a new window of exploration into the physiopathology of several bone diseases in which alterations of bone HA levels have been reported [16, 17].

4. Materials and Methods

4.1. Animal experiments

Hyal1 -/- mice (B6.129X1-*Hyal1*^{tm1Stn}/Mmucd) obtained from MMRRC (Mutant Mouse Resource Research Centers, USA) were raised in our laboratory and backcrossed for 9 generations on a C57BL/6 genetic background. All experimental procedures were approved by the Animal Ethics Committee of the University of Namur.

4.2. pQCT

Femurs from 1-year-old mice were cleaned of soft tissues, fixed in 10 % formalin for 48 h at RT and stored in 70 % EtOH at 4°C. The bone mineral density (BMD) was then determined by peripheral Quantitative Computed Tomography (pQCT) with a XCT Research Scanner. The BMD of the bones placed in a syringe filled with 70 % EtOH was measured at 17.5, 22 and 50 % from the distal end of the femurs. The slices had a thickness of 0.25 mm with a voxel size of 200 µm. The CALCBD program was used to analyze the trabecular and total BMD while the CORTBD function was used to assess the cortical BMD. In order to define trabecular bone, the outer 55 % of the bone cross section was concentrically excluded by the CALCBD function. Tissues with a density below 200 mg/cm^3 were removed as they were considered as soft tissues by the software. The cortical bone parameters were determined with a threshold setting of 350 mg/cm^3.

4.3. Osteoclast differentiation *in vitro*

Bone marrow monocytes were isolated from 7-month-old C57BL/6 male mice and cultured for 5 days in Minimum Essential Medium Eagle alpha modified media (α-MEM, Lonza) containing 10 % of inactivated FBS (Biological Industries), 1/10th volume of L929 cell culture supernatant which contains M-CSF [39], 2 mM glutamine (Lonza), 100 U/mL penicillin and 100 µg/mL streptomycin (Lonza). The cells were then trypsinized and split in individual wells. The differentiation process was induced by incubation with 20 ng/mL of RANKL (R&D Systems). The medium was replaced every other day. Experiments were conducted on day 7, unless specified otherwise.

4.4. TRAP staining of isolated osteoclasts

The cells were fixed for 30 sec in 4.6 mM citric acid, 2.3 mM sodium citrate, 3 mM NaCl, 65 % acetone and 3 % formaldehyde. After washing with H_2Od, the cells were incubated for 1 h at 37°C in 0.07 mg/mL Fast Garnet GBC (Sigma-Aldrich) previously diazotized for 2.5 min with 100 mM sodium nitrite, 0.13

mg/mL Naphthol AS-BI Phosphoric Acid (Sigma-Aldrich), 10 mM tartrate and 100 mM acetate buffer at pH 5.2. The cells were the washed with H_2Od and observed under a light microscope.

4.5. Actin ring staining and bone resorption assay

Bone marrow monocytes cultured in the presence of M-CSF for 5 days were plated onto thin nasal bovine bone slices (kindly provided by Dr. Haibo Zhao, Center for Metabolic Bone Diseases, University of Arkansas for Medicial Sciences). The differentiation into osteoclasts was then induced with RANKL as described above. 10 days later, the cells were fixed with 4 % of paraformaldehyde in PBS, permeabilized with PBS-saponin 0.5 % and incubated with 1 % of bovine serum albumin in PBS. The cells were then incubated for 15 min at RT with 5 % of Alexa 488-phalloidin in PBS (Invitrogen) and, after several washes in PBS, for 20 min at RT with 1 % of Hoechst 33258 in PBS (Molecular Probes). These probes label actin and nuclei, respectively. Osteoclasts with a minimum of 3 nuclei were counted with a BX63 Olympus fluorescence microscope prior to sonication of the bone slices in 1 M NaOH for 1 min. Soft brushing of the surface was subsequently conducted for 10 min in PBS containing 1 % of Triton X-100 and followed by an incubation of 1 min in 1 M NaOH to complete the removal of the cells. Lastly, the bone slices were washed in H_2Od, dehydrated in EtOH, dried and observed with a JEOL 6010LV scanning electron microscope to visualize resorption pits formed by osteoclasts.

4.6. ELISA assays

The following kits were used, following manufacturer's instructions: CrossLaps (CTX-I) ELISA kit, RatLaps (CTX-I) EIA kit, Rat/Mouse PINP EIA kit and Mouse TRAP5b ELISA kits (Immunodiagnostic Systems).

4.7. Western blotting

Cell lysates were prepared in PBS - Triton X-100 1 % (Sigma-Aldrich) and diluted in Laemmli's sample buffer containing 100 mM of DTT. Proteins from the serum-free conditioned media that were collected after a 4 h culture period were precipitated with 10 % trichloroacetic acid and mixed with Laemmli's sample buffer. The samples were then resolved by SDS-PAGE prior to protein transfer on Immobilon - FL PVDF membranes (Millipore). After blocking with 10 % fat-free milk in PBS-Tween 0.1 % for 1 h at RT, membranes were incubated overnight at 4°C with anti-cathepsin K (MAB3324, Millipore), anti-TRAP (SC-30833, Santa-Cruz Biotechnology) or anti-GAPDH (G8795, Sigma-Aldrich) antibodies diluted 1:1000 in 0.2 % fat-free milk in PBS-Tween 0.1 %. After washing with PBS-Tween 0.1 %, the membranes were incubated for 45 min at RT with the following fluorescent secondary antibodies diluted at 1:10 000 in 0.2 % fat-free milk in PBS-Tween 0.1 %: goat anti-mouse IgG IRDye 680RD and donkey anti-goat

IgG IRDye 800CW (LI-COR Biosciences). Lastly, the blots were washed, dried for at least 1 h and scanned with an Odyssey version 3.0 Imager (LI-COR Biosciences).

4.8. Quantitative PCR (qPCR)

Total RNA was extracted from cells using the High Pure RNA Isolation Kit (Roche) and reverse transcribed into cDNA with the RevertAid H Minus First Strand cDNA Synthesis Kit (Fermentas) following the manufacturer's protocols. qPCR was performed with the Takyon ROX SYBR MasterMix dTTP blue (Eurogentec) and a LightCycler 96 SW 1.1 system (Roche). Primers designed for the housekeeping gene *Gapdh* were used to normalize expression levels. The sequences of the primers that we used for each target can be found in Table 3. Fold changes ($2^{-\Delta\Delta CT}$) between samples for each gene were calculated from the average ΔCT values obtained from 5 mice in each group (with 2 replicates for each gene). To evaluate the statistical significance of the differences observed, a two-tailed Mann-Whitney U test was performed on ΔCT values, except when comparing osteoclasts with their precursor cells. In that case, the two-tailed Mann-Whitney U test was applied on ΔΔCT.

Protein / Gene name	Forward	Reverse
Cathepsin K / *Ctsk*	GAAGAAGACTCACCAGAAGCAG	TCCAGGTTATGGGCAGAGATT
CD44 / *Cd44*	TGGATCCGAATTAGCTGGAC	TACTATTGACCGCGATGCAG
GAPDH / *Gapdh*	CGTGCCGCCTGGAGAA	GATGCCTGCTTCACCACCTT
HYAL2 / *Hyal2*	CGA GGA CTC ACG GGA CTG	GGC ACT CTC ACC GAT GGT AGA
HYAL3 / *Hyal3*	CCG GAG CTC TGG GAG ATT C	GCG GCA CTC ACT CCA ATA GTC
TRAP / *Acp5*	GGTATGTGCTGGCTGGAAAC	ACGTGGAATTTTGAAGCGCAA

Table 3: Sequences (5'-3') of the primers used in qPCR.

4.9. Enzyme assays

To assay the phosphatase activity of TRAP, the samples were incubated at 37°C in 100 mM citrate buffer (pH 5.5) containing 50 mM sodium tartrate, 5 Units of heparin and 7.5 mM of para-nitrophenyl-phosphate (Sigma-Aldrich). Four hours later, the reaction was stopped by addition of 0.1 M glycine - NaOH at pH 10.6 and the absorbance was read at 405 nm.

4.10. Histology - Immunohistochemistry

Femurs were fixed with 4 % paraformaldehyde in PBS for 24 h at 4°C. The bones were successively washed with PBS, PBS-glycerol 5 %, PBS-glycerol 10 % and PBS-glycerol 15 % (12 h incubation in each solution, at 4°C). To decalcify the bones, the samples were incubated for 12 days at 4°C using 14.5 %

EDTA and 15 % glycerol at pH 7.3. The specimens were then washed with PBS-glycerol 15 %, PBS-glycerol 10 %, PBS-glycerol 5 % and PBS (12 h incubation in each solution, at 4°C). After a step of dehydration in methanol and toluol, the bones were embedded in paraffin and serially cut into 6 µm sections.

Sections were rehydrated and stained with hematoxylin eosin saffron (HES). The same procedure as described in the enzyme assay section was used to label TRAP followed by an hemalun staining on rehydrated bone tissue sections. To highlight HA, the sections were rehydrated, treated with 0.1 M glycine and with 3 % H_2O_2 followed by a blocking step of 1 h in PBS-BSA 0.2 % containing 0.02 % of Triton X-100. The slices were then incubated for 1 h at RT with a biotinylated Hyaluronic Acid Binding Protein (HABP, Calbiochem, 1:100 dilution), washed with PBS-BSA 0.2 %, and incubated for 1 h at RT with streptavidin-HRP (R&D Systems, 1:50 dilution). The 3,3'-diaminobenzidine technique (Liquid DAB + Substrate chromogen System, Dako) was used to reveal the signals.

4.11. Quantifications and statistics

Quantifications were made using the ImageJ program (Rasband, W.S., ImageJ, U. S. National Institutes of Health, Bethesda, Maryland, USA, http://imagej.nih.gov/ij/). Statistical analyses of the data were performed with the GraphPad Prism 5.0 program (GraphPad Software, Inc., La Jolla, USA). A two-tailed Mann-Whitney U statistical test was used. Results are presented as means ± standard error of the mean (SEM).

5. Acknowledgements

We thank Pr. Pascal Gustin (Fundamental and applied research for animals and health, University of Liège, Belgium) for granting us access to their pQCT machine. We are grateful to Dr. Haibo Zhao (Center for Metabolic Bone Diseases, University of Arkansas for Medical Sciences, USA), for the generous gift of bovine nasal bone slices. We thank Corry Charlier (Electron microscopy service, University of Namur, Belgium), Benoit Balau (Cell and tissue laboratory, University of Namur, Belgium) and Delphine Del Marmol (Cell and tissue laboratory, University of Namur, Belgium) for their technical help in the field of scanning electron microscopy and histological analyses. We are also thankful to Dr. Evgeni Ivanov and Dr. Todor Batakliev (OLEM, Institute of Mechanics, Bulgarian Academy of Sciences, Bulgaria) as well as Pr. Philippe Lambin (Physics of matter and radiation, University of Namur, Belgium) for their preliminary involvement in bone structure analyses.

References

[1] K.S. Girish, K. Kemparaju, The magic glue hyaluronan and its eraser hyaluronidase: a biological overview, Life Sci 80(21) (2007) 1921-43.
[2] R. Stern, Devising a pathway for hyaluronan catabolism: are we there yet?, Glycobiology 13(12) (2003) 105R-115R.
[3] L.Y. Bourguignon, P.A. Singleton, F. Diedrich, R. Stern, E. Gilad, CD44 interaction with Na+-H+ exchanger (NHE1) creates acidic microenvironments leading to hyaluronidase-2 and cathepsin B activation and breast tumor cell invasion, J Biol Chem 279(26) (2004) 26991-7007.
[4] B. Andre, C. Duterme, K. Van Moer, J. Mertens-Strijthagen, M. Jadot, B. Flamion, Hyal2 is a glycosylphosphatidylinositol-anchored, lipid raft-associated hyaluronidase, Biochem Biophys Res Commun 411(1) (2011) 175-9.
[5] M. Boonen, E. Puissant, F. Gilis, B. Flamion, M. Jadot, Mouse liver lysosomes contain enzymatically active processed forms of Hyal-1, Biochem Biophys Res Commun 446(4) (2014) 1155-60.
[6] E. Puissant, F. Gilis, S. Dogne, B. Flamion, M. Jadot, M. Boonen, Subcellular trafficking and activity of Hyal-1 and its processed forms in murine macrophages, Traffic 15(5) (2014) 500-15.
[7] H. Yoshida, A. Nagaoka, A. Kusaka-Kikushima, M. Tobiishi, K. Kawabata, T. Sayo, S. Sakai, Y. Sugiyama, H. Enomoto, Y. Okada, S. Inoue, KIAA1199, a deafness gene of unknown function, is a new hyaluronan binding protein involved in hyaluronan depolymerization, Proc Natl Acad Sci U S A 110(14) (2013) 5612-7.
[8] H. Yamamoto, Y. Tobisawa, T. Inubushi, F. Irie, C. Ohyama, Y. Yamaguchi, A mammalian homolog of the zebrafish transmembrane protein 2 (TMEM2) is the long-sought-after cell-surface hyaluronidase, J Biol Chem 292(18) (2017) 7304-7313.
[9] E.R. Bastow, S. Byers, S.B. Golub, C.E. Clarkin, A.A. Pitsillides, A.J. Fosang, Hyaluronan synthesis and degradation in cartilage and bone, Cell Mol Life Sci 65(3) (2008) 395-413.
[10] E.J. Chang, H.J. Kim, J. Ha, H.J. Kim, J. Ryu, K.H. Park, U.H. Kim, Z.H. Lee, H.M. Kim, D.E. Fisher, H.H. Kim, Hyaluronan inhibits osteoclast differentiation via Toll-like receptor 4, J Cell Sci 120(Pt 1) (2007) 166-76.
[11] E. Pivetta, M. Scapolan, B. Wassermann, A. Steffan, A. Colombatti, P. Spessotto, Blood-derived human osteoclast resorption activity is impaired by Hyaluronan-CD44 engagement via a p38-dependent mechanism, J Cell Physiol 226(3) (2011) 769-79.
[12] J. Salbach, S. Kliemt, M. Rauner, T.D. Rachner, C. Goettsch, S. Kalkhof, M. von Bergen, S. Moller, M. Schnabelrauch, V. Hintze, D. Scharnweber, L.C. Hofbauer, The effect of the degree of sulfation of glycosaminoglycans on osteoclast function and signaling pathways, Biomaterials 33(33) (2012) 8418-29.
[13] W. Ariyoshi, T. Takahashi, T. Kanno, H. Ichimiya, H. Takano, T. Koseki, T. Nishihara, Mechanisms involved in enhancement of osteoclast formation and function by low molecular weight hyaluronic acid, J Biol Chem 280(19) (2005) 18967-72.
[14] C.W. Lee, J.Y. Seo, J.W. Choi, J. Lee, J.W. Park, J.Y. Lee, K.Y. Hwang, Y.S. Park, Y.I. Park, Potential anti-osteoporotic activity of low-molecular weight hyaluronan by attenuation of osteoclast cell differentiation and function in vitro, Biochem Biophys Res Commun 449(4) (2014) 438-43.
[15] L. Huang, Y.Y. Cheng, P.L. Koo, K.M. Lee, L. Qin, J.C. Cheng, S.M. Kumta, The effect of hyaluronan on osteoblast proliferation and differentiation in rat calvarial-derived cell cultures, J Biomed Mater Res A 66(4) (2003) 880-4.
[16] A. Oohira, H. Nogami, Elevated accumulation of hyaluronate in the tubular bones of osteogenesis imperfecta, Bone 10(6) (1989) 409-13.
[17] I.R. Dickson, P.J. Roughley. The effects of vitamin D deficiency on proteoglycan and hyaluronate constituents of chick bone, Biochim Biophys Acta. 1181(1) (1993) 15-22.
[18] E. Puissant, M. Boonen, Monocytes/Macrophages Upregulate the Hyaluronidase HYAL1 and Adapt Its Subcellular Trafficking to Promote Extracellular Residency upon Differentiation into Osteoclasts, PLoS One 11(10) (2016) e0165004.
[19] C. Czupalla, H. Mansukoski, T. Riedl, D. Thiel, E. Krause, B. Hoflack, Proteomic analysis of lysosomal acid hydrolases secreted by osteoclasts: implications for lytic enzyme transport and bone metabolism, Mol Cell Proteomics 5(1) (2006) 134-43.
[20] M.R. Natowicz, M.P. Short, Y. Wang, G.R. Dickersin, M.C. Gebhardt, D.I. Rosenthal, K.B. Sims, A.E. Rosenberg, Clinical and biochemical manifestations of hyaluronidase deficiency, N Engl J Med 335(14) (1996) 1029-33.

[21] B. Triggs-Raine, T.J. Salo, H. Zhang, B.A. Wicklow, M.R. Natowicz, Mutations in HYAL1, a member of a tandemly distributed multigene family encoding disparate hyaluronidase activities, cause a newly described lysosomal disorder, mucopolysaccharidosis IX, Proc Natl Acad Sci U S A 96(11) (1999) 6296-300.
[22] L. Imundo, C.A. Leduc, S. Guha, M. Brown, G. Perino, L. Gushulak, B. Triggs-Raine, W.K. Chung, A complete deficiency of Hyaluronoglucosaminidase 1 (HYAL1) presenting as familial juvenile idiopathic arthritis, J Inherit Metab Dis 34(5) (2011) 1013-22.
[23] D.C. Martin, V. Atmuri, R.J. Hemming, J. Farley, J.S. Mort, S. Byers, S. Hombach-Klonisch, A.B. Csoka, R. Stern, B.L. Triggs-Raine, A mouse model of human mucopolysaccharidosis IX exhibits osteoarthritis, Hum Mol Genet 17(13) (2008) 1904-15.
[24] S. Tanaka, N. Takahashi, N. Udagawa, T. Tamura, T. Akatsu, E.R. Stanley, T. Kurokawa, T. Suda, Macrophage colony-stimulating factor is indispensable for both proliferation and differentiation of osteoclast progenitors, J Clin Invest 91(1) (1993) 257-63.H.
[25] H. Hsu, D.L. Lacey, C.R. Dunstan, I. Solovyev, A. Colombero, E. Timms, H.L. Tan, G. Elliott, M.J. Kelley, I. Sarosi, L. Wang, X.Z. Xia, R. Elliott, L. Chiu, T. Black, S. Scully, C. Capparelli, S. Morony, G. Shimamoto, M.B. Bass, W.J. Boyle, Tumor necrosis factor receptor family member RANK mediates osteoclast differentiation and activation induced by osteoprotegerin ligand, Proc Natl Acad Sci U S A 96(7) (1999) 3540-5.
[26] R. Hemming, D.C. Martin, E. Slominski, J.I. Nagy, A.J. Halayko, S. Pind, B. Triggs-Raine, Mouse Hyal3 encodes a 45- to 56-kDa glycoprotein whose overexpression increases hyaluronidase 1 activity in cultured cells, Glycobiology 18(4) (2008) 280-9.
[27] V. Atmuri, D.C. Martin, R. Hemming, A. Gutsol, S. Byers, S. Sahebjam, J.A. Thliveris, J.S. Mort, E. Carmona, J.E. Anderson, S. Dakshinamurti, B. Triggs-Raine, Hyaluronidase 3 (HYAL3) knockout mice do not display evidence of hyaluronan accumulation, Matrix Biol 27(8) (2008) 653-60.
[28] V. Bourguignon, B. Flamion, Respective roles of hyaluronidases 1 and 2 in endogenous hyaluronan turnover, FASEB J 30(6) (2016) 2108-14.
[29] J.R. Adams, G. Sander, S. Byers, Expression of hyaluronan synthases and hyaluronidases in the MG63 osteoblast cell line, Matrix Biol 25(1) (2006) 40-6.H.
[30] H. Zhao, T. Laitala-Leinonen, V. Parikka, H.K. Vaananen, Downregulation of small GTPase Rab7 impairs osteoclast polarization and bone resorption, J Biol Chem 276(42) (2001) 39295-302.
[31] K.H. Lau, T. Onishi, J.E. Wergedal, F.R. Singer, D.J. Baylink, Characterization and assay of tartrate-resistant acid phosphatase activity in serum: potential use to assess bone resorption, Clin Chem 33(4) (1987) 458-62.
[32] M. Shimoda, H. Yoshida, S. Mizuno, T. Hirozane, K. Horiuchi, Y. Yoshino, H. Hara, Y. Kanai, S. Inoue, M. Ishijima, Y. Okada, Hyaluronan-Binding Protein Involved in Hyaluronan Depolymerization Controls Endochondral Ossification through Hyaluronan Metabolism, Am J Pathol 187(5) (2017) 1162-1176.
[33] Y. Higuchi, Y. Nishida, E. Kozawa, L. Zhuo, E. Arai, S. Hamada, D. Morita, K. Ikuta, K. Kimata, T. Ushida, N. Ishiguro, Conditional knockdown of hyaluronidase 2 in articular cartilage stimulates osteoarthritic progression in a mice model, Sci Rep 7(1) (2017) 7028.
[34] A.R. Hayman, S.J. Jones, A. Boyde, D. Foster, W.H. Colledge, M.B. Carlton, M.J. Evans, T.M. Cox, Mice lacking tartrate-resistant acid phosphatase (Acp 5) have disrupted endochondral ossification and mild osteopetrosis, Development 122(10) (1996) 3151-62.
[35] P. Saftig, E. Hunziker, O. Wehmeyer, S. Jones, A. Boyde, W. Rommerskirch, J.D. Moritz, P. Schu, K. von Figura, Impaired osteoclastic bone resorption leads to osteopetrosis in cathepsin-K-deficient mice, Proc Natl Acad Sci U S A 95(23) (1998) 13453-8.
[36] P. Spessotto, F.M. Rossi, M. Degan, R. Di Francia, R. Perris, A. Colombatti, V. Gattei, Hyaluronan-CD44 interaction hampers migration of osteoclast-like cells by down-regulating MMP-9, J Cell Biol 158(6) (2002) 1133-44.
[37] J.J. Cao, P.A. Singleton, S. Majumdar, B. Boudignon, A. Burghardt, P. Kurimoto, T.J. Wronski, L.Y. Bourguignon, B.P. Halloran, Hyaluronan increases RANKL expression in bone marrow stromal cells through CD44, J Bone Miner Res 20(1) (2005) 30-40.
[38] W. Ariyoshi, T. Okinaga, C.B. Knudson, W. Knudson, T. Nishihara, High molecular weight hyaluronic acid regulates osteoclast formation by inhibiting receptor activator of NF-kappaB ligand through Rho kinase, Osteoarthritis Cartilage 22(1) (2014) 111-20.
[39] B.A. Scheven, J.S. Milne, S.P. Robins, A novel culture system to generate osteoclasts and bone resorption using porcine bone marrow cells: role of M-CSF, Biochem Biophys Res Commun 231(1) (1997) 231-5.

Fold increase	*Hyal1* -/- macrophages vs WT macrophages	*Hyal1* -/- osteoclasts vs WT osteoclasts	WT osteoclasts vs WT macrophages	*Hyal1* -/- osteoclasts vs *Hyal1* -/- macrophages
TRAP	1.91	1.36	1351.18	1509.65
Cathepsin K	1.10	1.60	669.99	818.02

Supplementary Table 1: Relative mRNA expression level of osteoclast markers TRAP and cathepsin K in osteoclasts and bone marrow monocytes isolated from WT or HYAL1 deficient mice (n = 5).